Bioprocess Biosyst Eng 25 (2002) 143–153
DOI 10.1007/s00449-002-0281-1

Scale-down studies on the hydrodynamics of two-liquid phase biocatalytic reactors

S.G. Cull, J.W. Lovick, G.J. Lye, P. Angeli

Abstract The maintenance of constant interfacial area per unit volume is a key parameter for the successful scale-up of two-liquid phase bioconversion processes. To date, however, there is little published information on the hydrodynamics of such systems and a suitable basis for scale-up has yet to be defined and verified. Here we report power input and hydrodynamic data for a whole-cell bioconversion process using resting cells of *Rhodococcus* R312 to catalyse the hydration of a poorly water-soluble substrate 1,3-dicyanobenzene (1,3-DCB). Experiments were performed in geometrically similar 3-L and 75-L reactors, each fitted with a three-stage Rushton turbine impeller system. The two-phase system used comprised of 20% v/v toluene dispersed in 0.1 M aqueous phosphate buffer containing up to 10 $g_{ww} \times L^{-1}$ of resuspended biocatalyst and 20 $g \times L^{-1}$ 1,3-DCB. The power input to the 3-L reactor was first determined using an air-bearing technique for both single-phase and two-phase mixing. In both cases, the power number attained a constant value of 11 at Re>10,000, while the measured power inputs were in the range 0.15–3.25 $kW \times m^{-3}$. Drop size distributions and Sauter mean drop diameters (d_{32}) were subsequently measured on-line in both reactors, using an in-situ light-backscattering technique, for scale-up on the basis of either constant power input per unit volume or constant tip speed. At both scales d_{32} decreased with increasing agitation rate, while the drop size distributions obtained were log-normal. All the measured d_{32} values were in the range of 30–50 μm, with the lowest values being obtained in systems with biocatalyst present. In all cases, constant power input per unit volume was found to be the most suitable basis for scale-up. This gave virtually identical d_{32} values and drop size distributions at both scales. A number of correlations were also identified that would allow reasonable prediction of d_{32} values for various agitation rates at each scale. While the results obtained are for a particular phase system, the scale-down methodology presented here would allow the rapid evaluation of other bioconversion processes in the 3-L reactor with a 25-fold reduction in scale. In this way, potential problems that might be encountered at the larger scale, such as the carryover of antifoam from the fermentation stage, could be quickly and efficiently identified.

Keywords Multiphase biocatalysis, Scale-down, Nitrile hydratase

Nomenclature

1,3-DCB	1,3-dicyanobenzene
C	Concentration ($g \times L^{-1}$)
c_1	Constant in Eq. 2 (dimensionless)
c_2	Constant in Eq. 2 (dimensionless)
D_i	Impeller diameter (m)
d_{max}	Maximum drop diameter (μm)
d_{32}	Sauter mean drop diameter (μm)
N	Rotational speed of the impeller (s^{-1})
P	Power (W)
Po	Power number: $Po=P/\rho N^3 D_i^5$ (dimensionless)
P/V	Power input per unit volume ($kW \times m^{-3}$)
Re	Reynolds number: $Re=\rho N D_i^2/\mu$ (dimensionless)
T	Tank diameter (m)
V	Liquid volume (m^3)
Vi	Viscosity group: $Vi=(\mu_d N D_i/\sigma)\ (\rho_c/\rho_d)^{0.5}$ (dimensionless)
We_T	Weber number: $We_T=\rho_c N^2 D_i^3/\sigma$ (dimensionless)

Greek symbols

ϕ	Volume fraction of dispersed phase: $\phi = V_d/V_{total}$ (dimensionless)
ρ	Density ($kg \times m^{-3}$)
σ	Interfacial tension ($kg \times s^{-2}$)
μ	Dynamic viscosity (Pa×s)

Subscripts

c	Continuous phase
d	Dispersed phase

Received: 2 August 2001 / Accepted: 17 January 2002
Published online: 24 May 2002

S.G. Cull, G.J. Lye
The Advanced Centre for Biochemical Engineering,
Department of Biochemical Engineering, University College London,
Torrington Place, London WC1E 7JE, UK

J.W. Lovick, P. Angeli (✉)
Department of Chemical Engineering, University College London,
Torrington Place, London WC1E 7JE, UK
E-mail: p.angeli@ucl.ac.uk

Financial support from the Biotechnology and Biological Sciences Research Council (BBSRC) is gratefully acknowledged. SGC and JWL would like to thank the BBSRC and EPSRC for the provision of research studentships. Both GJL and PA would like to thank Esso and the Royal Academy of Engineering for the award of Engineering Fellowships and GJL the Nuffield Foundation (NUF-NAL) for further financial support. The authors would also like to thank Raphael Santalucia for obtaining the power curve data for this study.

ex Experimental
lit Literature
m Mixture
ww Wet weight

1 Introduction

Biocatalysts are finding increasing use in the synthesis of chiral drugs and synthons, because they possess a number of significant advantages over chemical catalysts. These include high stereo- and regio-specificity, high atom efficiency (due to the avoidance of protection and deprotection steps) and the ability to operate under mild conditions. In many cases, the substrates and/or products of interest have relatively low water solubilities, being typically less than 0.5 g×L^{-1}. This has led to the development of aqueous-organic, two-liquid phase reaction media to effect bioconversions at higher overall concentrations and to overcome issues of substrate and product inhibition [1]. A number of such processes have now been operated commercially [2].

Currently, there is little information available on the hydrodynamics and phase behaviour of two-phase bioconversion processes carried out in stirred-tank reactors. Knowledge of the droplet size distribution, in particular, is critical for estimation of the interfacial area and hence the rate of solute transfer between the phases. To date, however, little is known on how the droplet size distribution varies as a function of reactor design and operation, while none of the suggested scale-up criteria are generally accepted [3]. From a hydrodynamic standpoint, two-phase bioconversion processes can be classified according to the metabolic state of the biocatalyst:

1. Processes employing growing cells: bioconversions requiring actively growing cells necessitate the use of complex growth media and frequently result in the production of extracellular, surface-active metabolites as a consequence of solvent exposure throughout the fermentation [4]. Recent results have shown that droplet coalescence is hindered in such systems and that the equilibrium drop size distribution is primarily determined by the surface activity of the broth components rather than the agitation conditions [5]. These processes are also likely to require the supply of a gaseous substrate such as oxygen.
2. Processes employing resting cells: bioconversions using resting cells (or immobilised enzymes) are generally carried out in simpler systems in which the cells are first recovered from the fermentation broth and then resuspended in a simple aqueous buffer. The substrate-containing solvent phase is then added to begin the bioconversion. In these processes, unless the substrate or product molecules are surface active, the equilibrium drop size distribution should primarily be determined by the agitation conditions. Unless a redox enzyme is involved, the supply of gaseous oxygen is not necessarily required.

In bioconversions employing resting cells the drop size distribution will thus be primarily determined by the competing phenomena of drop break-up and coalescence. From the different suggested mechanisms, break-up in the inertial subrange of turbulence will be the prevailing one in dilute dispersions [6]. The maximum drop size that can resist break-up, d_{max}, will depend on the balance between the stresses generated by external turbulent fluctuations, which tend to break the drops, and surface tension, which tends to stabilise them [7]. In a stirred vessel d_{max} will be given by

$$d_{max}/D_i \propto We_T^{-0.6} \quad (1)$$

where We_T is the stirred-tank Weber number [3]. The maximum droplet size is thus determined by the continuous-phase density, ρ_c, the impeller rotational speed, N, the impeller diameter, D_i, and the interfacial tension, σ. The dispersed-phase viscosity can help stabilise the drops and its effect is often accounted for by introducing a viscosity number. This can, however, be ignored for systems with small viscosity differences between the phases.

Coalescence of drops will occur at high dispersed-phase volume fractions and will result in increased drop sizes. The mechanisms relevant to drop-drop coalescence have been detailed by Chesters [8]. However, even when coalescence is prevented, increasing the volume fraction of the dispersed phase will decrease the turbulence intensity and, therefore, increase the dispersed-phase droplet size. To account for the effect of volume fraction on d_{max}, investigators have used a linear concentration correction function with the general form:

$$d_{max}/D_i = c_1(1 + c_2\phi)We_T^{-0.6} \quad (2)$$

where D_i is the impeller diameter, c_1 and c_2 are constants and ϕ is the volume fraction of the dispersed phase. Instead of d_{max}, a more useful parameter, particularly for mass transfer operations, is the Sauter mean diameter, d_{32}, which is often assumed to be proportional to d_{max} (though this has recently been questioned [9]). A number of correlations taking the form of Eq. 2 have been proposed in

Table 1. Literature correlations for the prediction of Sauter mean drop diameter in agitated liquid-liquid systems (compiled from [3]); *RT* Rushton turbine

Author	Correlation equation	D_i (cm)	T (cm)	ϕ	Impeller characteristics
Chen and Middleman 1967 [25]	$d_{32}/D_i = 0.053(We_T)^{-0.6}$	5.1–15.2	10–45.7	0.001–0.005	Single 6-bladed RT
Brown and Pitt 1972 [30]	$d_{32}/D_i = 0.051(1+3.14\phi)(We_T)^{-0.6}$	10	30	0.05–0.3	Single 6-bladed RT
Van Heuven and Beek 1971 [28]	$d_{32}/D_i = 0.047(1+2.5\phi)(We_T)^{-0.6}$	3.75–40	12.5–120	0.04–0.35	Single 6-bladed RT
Wang and Calabrese 1986 [31]	$d_{32}/D_i = 0.053(We_T)^{-0.6}\times (1+0.97Vi^{0.79})^{0.6}$	7.1–19.6	14.2–39.1	<0.005	Mainly single 6-bladed RT
Godfrey and Grilc 1977 [26]	$d_{32}/D_i = 0.058(1+3.6\phi)(We_T)^{-0.6}$	5.1	15.2	0.05–0.5	Single 6-bladed RT

the literature and some of those most relevant to this work are given in Table 1. The constant c_2 is considered equal to 3 when it accounts for turbulence damping at low dispersed-phase concentrations [10], or higher than 3 for coalescing systems [9]. Equation 2 predicts an increase in the drop size with increasing dispersed-phase volume fraction. At high dispersed-phase volume fractions (usually above 40%), however, a further increase in the dispersed concentration results in decreasing drop size [6, 11]. This behaviour has been attributed to alternative mechanisms of drop break-up for Reynolds numbers below 1,000 [6] but is not relevant to the work performed here.

The existing scale-up literature for two-liquid phase reactors mainly relates to simple chemical systems. Scale-up has tended to focus on the maintenance of a constant interfacial area per unit volume. The two most popular criteria for scale-up in geometrically similar liquid-liquid agitated systems are constant power input per unit volume (P/V) and constant impeller tip speed, respectively [12]. Podgorska and Baldyga [13] recently proposed that the fluid circulation time in the vessel is also relevant and considered instead the following four criteria for scale-up: (i) equal power input per unit mass and geometric similarity, (ii) equal average circulation time and geometric similarity, (iii) equal power input per unit mass, equal average circulation time and no geometric similarity, (iv) equal impeller tip speed and geometric similarity. The study demonstrated that in fast coalescing systems both criteria (i) and (iii) resulted in small changes in the drop size distribution during scale-up, while in slow coalescing systems none of the criteria seemed to perform satisfactorily.

Literature on the scale-up of complex two-liquid phase bioconversion processes is extremely limited. Previous investigators have simply indicated that during scale-up consistency should be maintained in all reactor conditions and have postulated that scale-up on the basis of constant P/V was appropriate [14]. In the current paper, detailed results on the scale-up and hydrodynamics of a two-phase bioconversion process using a resting whole-cell biocatalyst are reported for the first time. Experiments were performed in two geometrically similar 3-L and 75-L reactors, while the dynamic variation of droplet size distribution, as a function of power input and reactor size, was measured on-line using a light-backscattering technique. For scale-up, the two commonly used criteria of constant P/V and constant impeller tip speed were investigated. The whole-cell bioconversion studied used resting cells of *Rhodococcus* R312 to catalyse the hydration of 1,3-dicyanobenzene (1,3-DCB) to 3-cyanobenzamide. The selection of organic phases for the solubilisation of 1,3-DCB and the optimisation of transformation conditions have been previously reported [15].

2 Materials and methods

2.1 Materials

The substrate 1,3-DCB, the organic solvent toluene and all other chemicals were purchased from Sigma-Aldrich Chemical Co. (Dorset, UK) and were of the highest purity available.

2.2 Microorganism, growth medium and cultivation

The microorganism used, *Rhodococcus* R312, was a kind gift from Professor N. J. Turner (University of Edinburgh, UK) and was stored on nitrile-metabolising agar at 4°C [16]. Cells for small-scale (3 L) experiments were produced by multiple shake-flask fermentations (200 mL) using a growth medium containing 30 g×L^{-1} tryptic soy broth (TSB) in deionized water. The fermentations were carried out in 2-L baffled conical flasks in a shaking incubator operated at 200 rpm and 30°C. Cells were subsequently harvested by batch centrifugation at the end of the exponential growth phase (this was typically 40 h after inoculation at an OD_{600} of 12) and were resuspended in 0.1 M phosphate buffer, pH 7, before use.

Cells for large-scale (75 L) experiments were produced in a 450-L Chemap AG (Volketswil, Switzerland) stirred-tank fermenter fitted with a three-stage Rushton turbine impeller system [17]. The inoculum chain involved production of 15 L of inoculum in an Inceltech 20-L fermenter using 30 g×L^{-1} TSB in deionized water (4 mL of PPG antifoam was added initially to prevent foaming). This fermenter was operated at 30°C and 500 rpm with an aeration rate of 0.5 vvm and was harvested after 31 h at an OD_{600} of 16. The Inceltech fermenter was itself initially inoculated with 250 mL of *Rhodococcus* R312 broth prepared by shake-flask fermentations as described above. To begin the fermentation in the 450-L vessel, the 15-L inoculum was aseptically pumped into the fermenter, which was pre-filled with 285 L of sterile TSB medium containing 60 mL PPG. The fermentation in the 450-L vessel was then performed at 30°C and 180 rpm with an aeration rate of 0.5 vvm and was harvested after 16 h at an OD_{600} of 16. In all fermentations, pH was kept constant at pH 7 by the controlled addition of 4 M NaOH and/or 4 M phosphoric acid. Exit gas data was obtained using a VG Prima mass spectrometer (VG Gas Analysis Ltd., Cheshire, UK).

The 300 L of fermentation broth from the Chemap fermenter was processed through a Carr Powerfuge (Franklin, Mass., USA) to recover the biomass from the liquid fermentation medium. The Powerfuge was operated at 15,200 rpm with a feed flow rate of 1 L×min^{-1} and 50-L batches of broth were processed at a time. In total, 3.6 kg of biomass in dry solid form was recovered and stored in polythene bags at 4°C for subsequent use in 75-L-scale bioconversion experiments (see reference [17] for full details of fermentation conditions).

2.3 Bioreactor geometry and operation

The two-phase bioconversion experiments were carried out in two geometrically similar stirred-tank reactors, each fitted with a stainless steel, three-stage, six-bladed Rushton turbine impeller system (Fig. 1). The Inceltech LH SGI (Wokingham, UK) 75-L stainless steel solvent reactor was operated in a dedicated pilot plant facility designed according to both solvent and biological containment regulations. The 3-L scale-down reactor was of glass

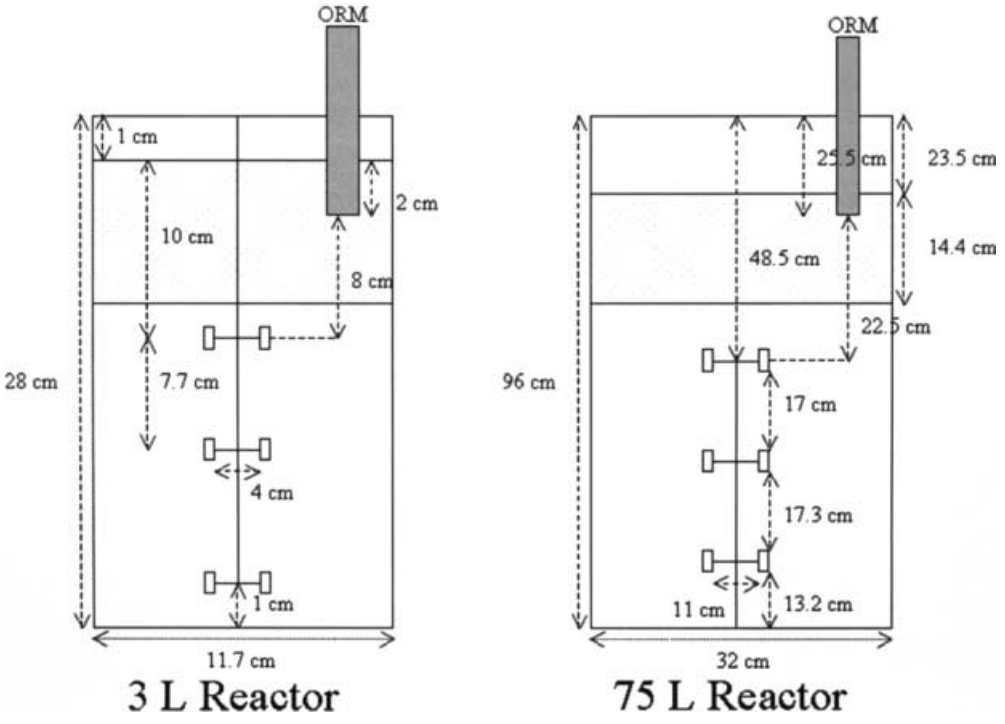

Fig. 1. Schematic diagrams of the 3-L scale-down reactor and 75-L pilot-scale reactor used in this work

construction and was operated in a fume hood. Although different rates of coalescence at the equipment surface (reactor walls) may be expected due to the different materials of construction, any such effects are assumed to be minimal. To minimise the risk of explosion, the impeller in the 3-L reactor was rotated using an air-driven, spark-proof motor. In the 75-L reactor a constant positive pressure of nitrogen was maintained in the headspace to exclude any oxygen. Both vessels were thoroughly cleaned and rinsed with deionised water between runs. The temperature in both reactors was maintained constant at 30±0.2°C in all experiments.

2.3.1
Power consumption and phase continuity

Power consumption was measured during the agitation of single-phase and two-phase liquid systems in the 3-L reactor. For the two-phase experiments, the phase continuity was also monitored using a micro-conductivity probe, made in-house, connected to an Alpha 800 conductivity meter (Courtcloud Ltd, UK). This minimised the disturbance of the flow field during measurements. For power consumption measurements, the entire vessel was placed on a turntable supported on an air layer (air bearing technique). During agitation the force required to stop the rotation of the vessel on the frictionless air bearing was recorded with a load cell and the power input into the vessel was calculated. Full details can be found in reference [17]. All experiments were performed in triplicate with the maximum coefficient of variance for the calculated power input being 2.7%.

For two-phase system experiments, the vessel was first carefully filled with the aqueous phase followed by the organic phase, at the appropriate volume fraction, and agitation was then started. Initial experiments had showed that 600 rpm was the minimum rotational speed necessary to ensure complete dispersion of the organic phase at all the volume fractions tested, i.e. no organic layer remained at the surface of the dispersion. Power measurements were recorded after 30 min of operation, to ensure that the system had reached steady state, for agitation rates varying from 650 to 1,100 rpm. Drop size measurements, as described in Sect. 2.3.2, confirmed that a steady-state droplet size had been reached after this time. In these experiments, both pristane (2,6,10,14-tetramethylpentadecane) and toluene were used as the organic phase, with their volume fractions varying between 10–90% and 10–30%, respectively.

2.3.2
On-line measurement of drop size distributions

Drop size distributions were recorded using an Optical Reflectance Measurement (ORM) particle size analyser (MTS, Düsseldorf, Germany) that can provide in-situ and on-line measurements. The technique uses a laser beam which, through a lens, is focused a short distance in front of the probe tip to a high-intensity focal point and is rotated at a known velocity within the sample. When the rotating beam intercepts a drop, light is scattered back, through the optical system of the instrument, to a detector and the chord length of the drop is determined. Measurements over a period of time will produce a distribution of drop chord lengths. This is then transformed to a drop diameter distribution using a calibration curve and assuming that the drops are spherical. Since the laser beam is focused only at a short distance away from the instrument and does not pass through the dispersion, the measurements are not limited by the dispersed-phase concentration [18], a common problem with other light-based drop size analysers. As the technique can also be used in-situ, it does not require any manipulation of the dispersion before the measurement. The ORM instrument

has previously been used in various aqueous-organic systems, where it has been found to respond swiftly to any changes in process conditions that affect drop size [19, 20, 21]. In this work, the calibration of the ORM instrument was set using a drop size distribution calibration curve obtained with a Malvern Mastersizer 3600 (E-Type, Malvern Instruments Ltd., Worcester, UK). A series of standard size microspheres (Polymer Laboratories, UK) was then used to check the satisfactory calibration of the ORM instrument before use.

For drop size distribution experiments, the ORM probe tip was mounted vertically at approximately the same position in both the 3-L and 75-L reactors as indicated in Fig. 1. Droplet size distributions were measured in the 3-L reactor for a 20% v/v toluene-aqueous system agitated between 600 and 900 rpm. The effect of the addition of 20 $g \times L^{-1}$ 1,3-DCB (in toluene) with and without 10 $g_{ww} \times L^{-1}$ of the biocatalyst (in the aqueous phase) was also examined. All experiments were performed in triplicate, with the maximum coefficient of variance for the measured steady-state mean drop size being 3%. Droplet size distributions were further analysed in the 75-L reactor (60 L total liquid volume) for a 20% v/v toluene-aqueous system with and without biomass present. The agitation rates used corresponded to scale-up on the basis of constant power input per unit volume or constant tip speed as shown in Table 2. A viewing window, running the full height of the 75-L vessel, enabled visual confirmation that no organic layer remained on the surface of the dispersion even at the lowest impeller speeds used. In both reactors using 'clean' phase systems (biomass-free), the two phases were mixed at the designated speed for 15 min before measurements commenced. Drop size distributions were then recorded every 60 s for a further 20 min. For experiments with the biocatalyst present, drop size distributions were recorded as soon as mixing of the phases commenced and continued over a period of 100 min. These times were chosen since previous work had shown that the bioconversion would have reached completion by this time.

Table 2. Reactor agitation rates at 3-L and 75-L scales for scale-up using constant power input per unit volume and constant tip speed criteria

Agitation rate at 3-L scale (rpm)	Agitation rate at 75-L scale (rpm)	
	P/V constant ($N^3D_i^2$=constant)	Tip speed constant (ND_i=constant)
600	305	218
700	357	255
800	408	291
900	459	328

2.4 Analytical techniques

The densities of the liquid phases used were determined gravimetrically. Liquid viscosity was measured using a Contraves Rheomat 115 (Contraves AG, Zurich, Switzerland). Surface tension and interfacial tension were measured using a Kruss K12 process tensiometer. The final values recorded were the average of three replicate measurements in each case. Further details on all techniques can be found in reference [17].

3 Results and discussion

3.1 Phase physical properties

The main organic solvent used in the present study, toluene, had been selected in earlier solvent-screening studies [15]. These showed that toluene solubilised relatively high concentrations of the 1,3-DCB substrate (~25 $g \times L^{-1}$) and was reasonably biocompatible with the *Rhodococcus* R312 catalyst. The aqueous phase used consisted of 0.1 M potassium phosphate buffer which, at pH 7, provided the optimal conditions for nitrile hydratase activity. Table 3 summarises the physical properties of the individual phases used in the current work.

For a 'clean' biphasic system (i.e. in the absence of substrate or biomass) of toluene-aqueous buffer, an interfacial tension of 0.035 $kg \times s^{-2}$ was determined. This is similar to values reported by previous investigators for a variety of model systems that had interfacial tension values between 0.002 and 0.050 $kg \times s^{-2}$ [3]. The addition of substrate, 1,3-DCB, to the toluene phase had no apparent effect on the physical properties of the solvent or the measured interfacial tension at concentrations up to 20 $g \times L^{-1}$. In contrast, the addition of 10 $g_{ww} \times L^{-1}$ of biomass to the aqueous phase was found to significantly reduce the interfacial tension to a value of around 0.0013 $kg \times s^{-2}$. This low value is most likely due to the adsorption of biomass at the interface, but may also be the result of small amounts of media components, especially antifoam, still present in the system after harvesting and resuspension of the biomass. It should be noted that adsorption of the biomass at the interface made accurate measurements of the interfacial tension difficult. The implications of the reduced interfacial

Table 3. Experimentally determined phase physical properties. Measurements performed as described in Sect. 2.4

Physical property	Phase composition		
	Aqueous phosphate buffer	Aqueous phosphate buffer plus 10 $g_{ww} \times L^{-1}$ biocatalyst	Toluene
Formula	KH_2PO_4/K_2HPO_4	KH_2PO_4/K_2HPO_4	$C_6H_5CH_3$
Molecular weight	328	328	92
Density ($kg \times m^{-3}$)	1,011±5	1,034±6	857±3
Dynamic viscosity ($mPa \times s$)	1.274±0.03	1.321±0.006	0.51±0.02
Surface tension ($kg \times s^{-2}$)	71.9±0.05	34.9±0.5	28.1±0.3

tension on drop size distributions will be illustrated later.

3.2
Power curves for agitated liquid-liquid systems (3-L scale)

The power input for a homogenous liquid agitated in a tank fitted with a single Rushton turbine impeller can easily be found in the literature. For the particular tank and turbine geometry used in this work, however, it was necessary to determine the power number, *Po*, experimentally. In general, when more than one impeller is used, *Po* will depend on the number of impellers, the spacing between them and the clearance of the lower impeller from the bottom of the vessel [22]. For agitation of each of the 'clean' homogeneous phases used here, it was found that the power number acquired a constant value of 11 for Reynolds numbers above 10,000 (data not shown). The measured power inputs for agitation rates of 400–1,200 rpm were between 0.5 and 3.25 $kW \times m^{-3}$.

The power consumption was also measured during two-phase mixing, using both toluene and pristane as the solvent phase. Pristane (ρ=790 $kg \times m^{-3}$, μ=5 mPa×s) is a solvent with a high log-P value, widely used in two-phase biotransformation processes, and was initially investigated as an alternative to toluene. The power consumption results are shown in Fig. 2 as *Po* against *Re* for both systems over a range of solvent volume fractions. For the determination of *Re* in the biphasic systems, volume-averaged density values were used, while viscosity values were calculated using:

$$\mu_m = \frac{\mu_c}{1-\phi}\left(1 + \frac{1.5\phi\mu_d}{\mu_c + \mu_d}\right) \quad (3)$$

where, ϕ is the volume fraction of the dispersed phase and μ_c and μ_d are the viscosities of the continuous and the dispersed phase, respectively [23]. In this case, the measured power inputs were slightly lower than for the single-phase systems being in the range 0.15–2.31 $kW \times m^{-3}$ for agitation rates of 650–1,100 rpm.

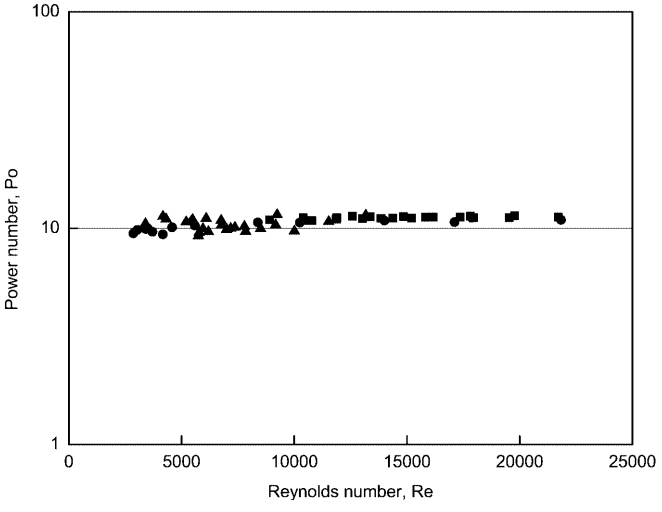

Fig. 2. Power curves for a variety of agitated two-liquid phase systems. Power measurements were made in the 3-L scale-down reactor for 10–30% v/v toluene-aqueous and 10–90% v/v pristane-aqueous systems mixed at agitation rates of 650–1,100 rpm as described in Sect. 2.3.1

Po is again seen to be constant and equal to 11 for agitation at Reynolds numbers above 10,000, similar to the case of single-phase systems. Reynolds numbers larger than 10,000 were achieved for water-continuous mixtures with dispersed-phase volume fractions up to 30%. For the more concentrated water-continuous dispersions, and for oil-continuous dispersions, *Re* values fell below 10,000 and *Po* was less than 11. Our previous experiments have investigated conditions to optimise the biocatalytic hydration of 1,3-DCB using toluene as the solvent phase at volume fractions between 5 and 30% [15]. A phase system comprising 20% v/v toluene and 80% v/v aqueous buffer containing 10 $g_{ww} \times L^{-1}$ of biocatalyst was found to be most suitable as this maximised the synthesis of the 3-cyanobenzamide product and minimised the damaging effect of the toluene on the biocatalyst. Scale-up and droplet size distribution studies were thus performed solely with this system.

3.3
Effect of agitation rate and phase composition on drop size distributions (3-L scale)

Drop size distributions were initially measured in the 3-L scale-down reactor to examine the influence of agitation rate and phase composition on drop size distribution and Sauter mean drop diameter. Figure 3a shows that increasing the agitation rate in a 'clean' 20% v/v toluene-aqueous system resulted in narrower drop size distributions, shifted to smaller droplet sizes. The distributions shown were recorded 15 min after mixing began, although the distributions did not change significantly from 10 min onwards. The addition of 20 $g \times L^{-1}$ 1,3-DCB to the toluene phase produced no significant change in the measured size distributions or the Sauter mean diameters (data not shown). As stated previously, addition of the substrate did not alter the physical properties of the toluene phase or the interfacial tension of the biphasic system.

Figure 3b, however, shows that the addition of 10 $g_{ww} \times L^{-1}$ of biocatalyst to the aqueous phase shifted the measured distribution to smaller drop sizes. The individual *Rhodococcus* R312 cells are approximately 1 μm in diameter; this is below the detection limit of the ORM instrument and hence they are not registered in the size distribution. The reduction in droplet size with biomass present is attributed to the significantly reduced interfacial tension as described in Sect. 3.1. The difference between the droplet size distributions in the presence and absence of biomass decreased with increasing agitation rate (data not shown). In all cases, the measured drop sizes could be adequately described by a log-normal distribution, as indicated in Fig. 3b for an agitation rate of 600 rpm. These distributions show a 'tail' at the large end of the drop size spectrum. Mixing of the two phases with biomass present also led to the formation of a stable inter-phase after phase separation. Visually, the system comprised of clear upper (toluene) and lower (aqueous buffer) phases with an inter-phase of cells present between them.

Figure 4 shows the Sauter mean drop diameters, determined from the drop size distribution data, at agitation

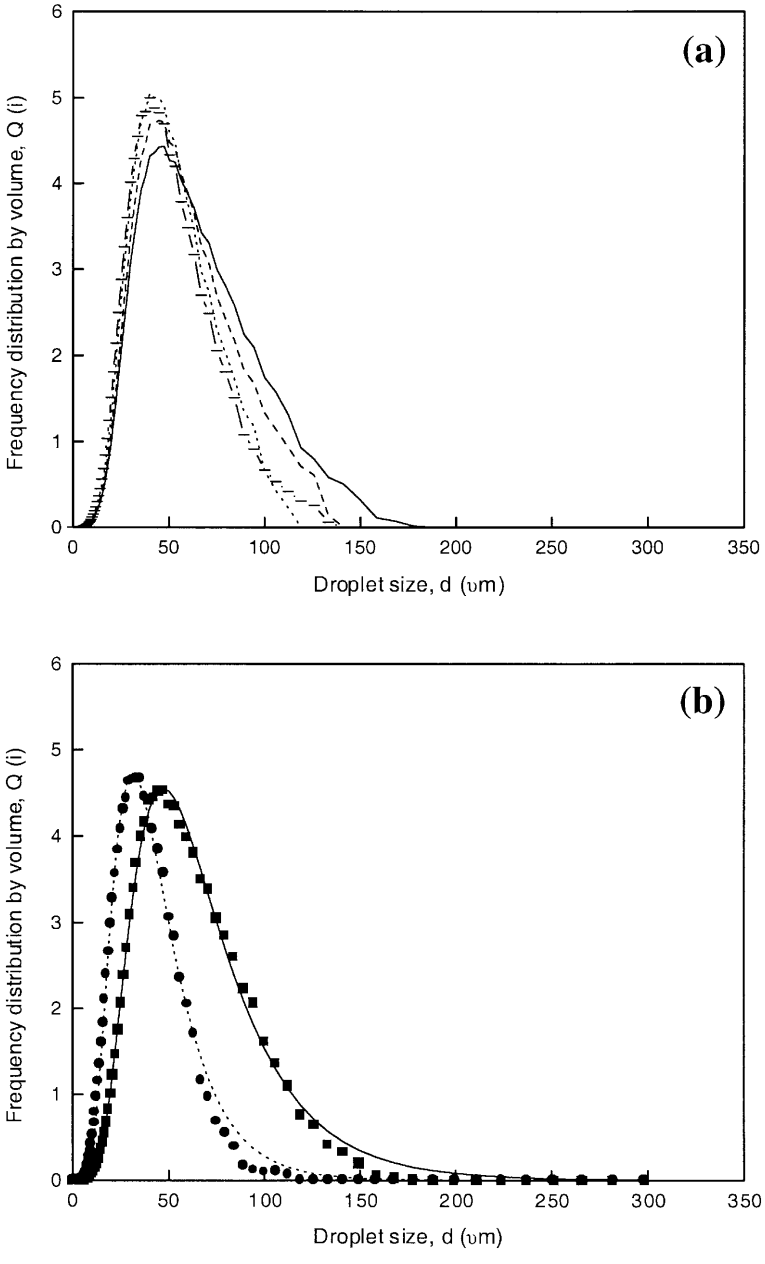

Fig. 3. **a** Droplet size frequency distribution by volume as a function of agitation rate for a 20% v/v toluene-aqueous system in the 3-L reactor in the absence of substrate and biomass: (__) 600 rpm; (_ _) 700 rpm; (....) 800 rpm; (–) 900 rpm. **b** Droplet size frequency distribution by volume for a 20% v/v toluene- aqueous system agitated at 600 rpm in the 3-L reactor: (■) no substrate or biomass present; (●) 10 $g_{ww} \times L^{-1}$ biomass present. *Lines* show fitted log-normal distributions. Droplet size measured as described in Sect. 2.3.2

rates between 600 and 900 rpm for both 'clean' and biomass-containing phase systems. As expected from the distribution data, the Sauter mean drop size is seen to decrease slightly with increasing agitation rate from 42 to 36 μm in the 'clean' system and from 31 to 27 μm in the system with biomass. It is difficult, however, to compare the magnitude of the drop sizes recorded with literature values due to the limited amount of published data and the rather different phase compositions and reactor geometries studied. Galindo et al. [24] investigated droplet sizes in systems with up to four phases present for a highly viscous castor oil (μ=560 mPa×s) dispersed in an aqueous salt solution. Experiments were performed at an agitation rate of 250 rpm in a tank fitted with a single Rushton turbine impeller. The drop sizes recorded using an in-situ video technique were between 750 and 1,250 μm for oil volume fractions between 2 and 16%. These very large drop sizes are in contrast to those reported by Schmid et al. [4], who measured drop sizes of 10–13 μm using an off-line laser refraction spectrometer in a 1.4-L 20% v/v decane-water system containing 1 $g \times L^{-1}$ biosurfactant. These experiments were performed in a 3-L reactor fitted with two Rushton turbine impellers operated at agitation rates of 1,500–2,500 rpm. Clearly, the Sauter mean drop sizes reported here lie somewhere between these two extremes and can be explained by the different agitation conditions, fluid properties and methods of drop size analysis used.

3.3.1
Prediction of Sauter mean drop diameter

For process design purposes, it is useful to be able to predict Sauter mean drop sizes and how these vary with reactor operation. Figure 4 also shows the comparison between experimental d_{32} values and those predicted using the literature correlations detailed in Table 1. These particular correlations were chosen from the many available

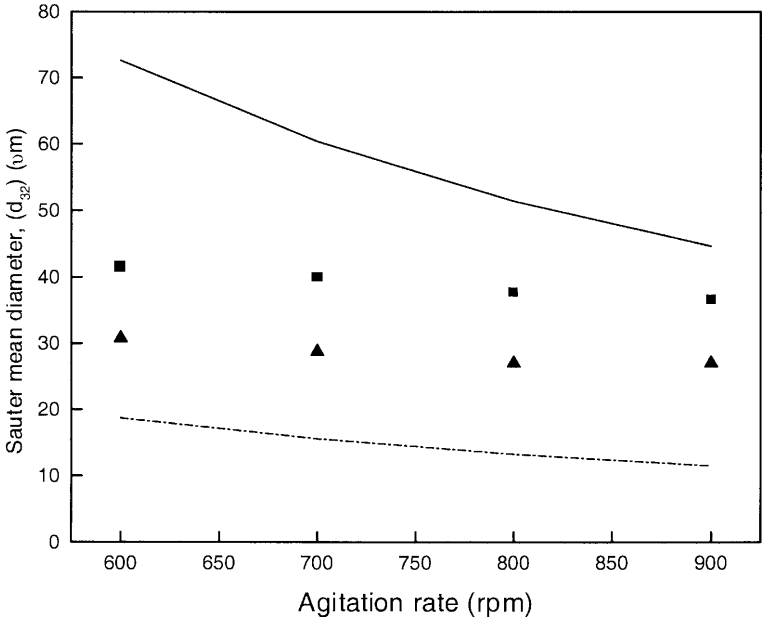

Fig. 4. Sauter mean diameter (d_{32}) against agitation rate in 20% v/v toluene-aqueous systems in the 3-L reactor (■) without biomass present and (▲) with 10 $g_{ww} \times L^{-1}$ biomass present. *Lines* show predicted d_{32} values using correlations from Table 1 corrected for increased power input: (*solid line*) Chen and Middleman [25] predictions for the biomass-free system; (*dashed line*) Godfrey and Grilc [26] predictions for the biomass-containing system

as they were derived in systems with phase physical properties most similar to the ones used in this work. The majority take the general form previously shown in Eq. 2. However, virtually all were developed in vessels fitted with a single Rushton turbine impeller (Po=6). In the current work, a three-stage Rushton turbine impeller was used which results in a higher power input for the same agitation rate or higher Po values (see Fig. 2). In order to account for this difference in power input and for the different tank geometry compared to the standard configuration used in most studies, the $(We_T)^{-0.6}$ term in the equations in Table 1 was substituted by

$$We_T^{-0.6}\left(\frac{Po_{\text{lit}}}{Po_{\text{ex}}}\right)^{0.4}\left(\frac{\beta_{\text{ex}}}{\beta_{\text{lit}}}\right)^{0.4} \quad (4)$$

where β is the ratio of V/D_i^3, Po_{lit} is equal to 6 for a single Rushton turbine and Po_{ex} is equal to 11, as experimentally determined in Sect. 3.2 [17].

The predicted d_{32} values shown in Fig. 4 are for the correlations with the closest predictions to the experimental values. For the 'clean' system, the Chen and Middleman [25] correlation was found to be the most appropriate. This overpredicted the experimental values by 25–78%. This is probably due to the larger number of impellers used in this work. Generally, in stirred tanks, drops break up in the impeller region and coalesce in regions further away. In the correlations for d_{32} or $d_{\max}$, the average energy dissipation rate is used, which includes both these regions. In our reactor, however, the use of three impellers decreases significantly the size of the coalescence region, which would be expected to lead to smaller drop sizes than those predicted. Further work on the variation of drop size at different locations in the reactor would provide useful insight. For the system with biomass present, the Godfrey and Grilc correlation [26] was most appropriate, although this underpredicted the experimental values by 39–59%. This underprediction could be a consequence of the very low interfacial tension measured (Sect. 3.1) or the stabilisation of the drops by surface-active agents, which could be present. It is also possible that the actual interfacial tension in the reactor is somewhat larger than measured at equilibrium in the static system due to the kinetics of biomass adsorption on the droplets during the course of the experiment. These results indicate that, although reasonable drop size predictions can be made, further work is required to develop more accurate correlations for this typical reactor geometry widely used with biological two-phase systems.

Interestingly, it was also found that when d_{32} was plotted against We, the exponent on We was larger than the commonly used value of (–0.6). Similar findings, reported by other investigators recently [27, 10], could imply that the mechanism of break-up in a turbulent dispersion is different than that originally suggested by Hinze [7]. Drop break-up mainly occurs in the impeller region, where the isotropic turbulence assumption of the Hinze theory least applies. The limited range of impeller speeds and dispersed-phase volume fractions used in this work, however, does not allow any conclusions to be drawn in this respect.

3.4
Criteria for reactor scale-up to 75-L scale

As mentioned earlier, the maintenance of constant power input per unit volume (or $N^3D_i^2$=constant) and constant tip speed (or ND_i=constant) were the two criteria used here for scale-up from the 3-L to the 75-L reactor. The respective agitation rates for scale-up using these two criteria are given in Table 2. Although the inclusion of the circulation time (as suggested in reference [13]) is an interesting concept when considering scale-up, its application is limited due to the difficulty in defining this parameter [3]. Droplet size distributions were again measured in the 75-L reactor for both a 'clean' 20% v/v toluene-aqueous buffer system and one in which 10 $g_{ww} \times L^{-1}$ of biomass was present.

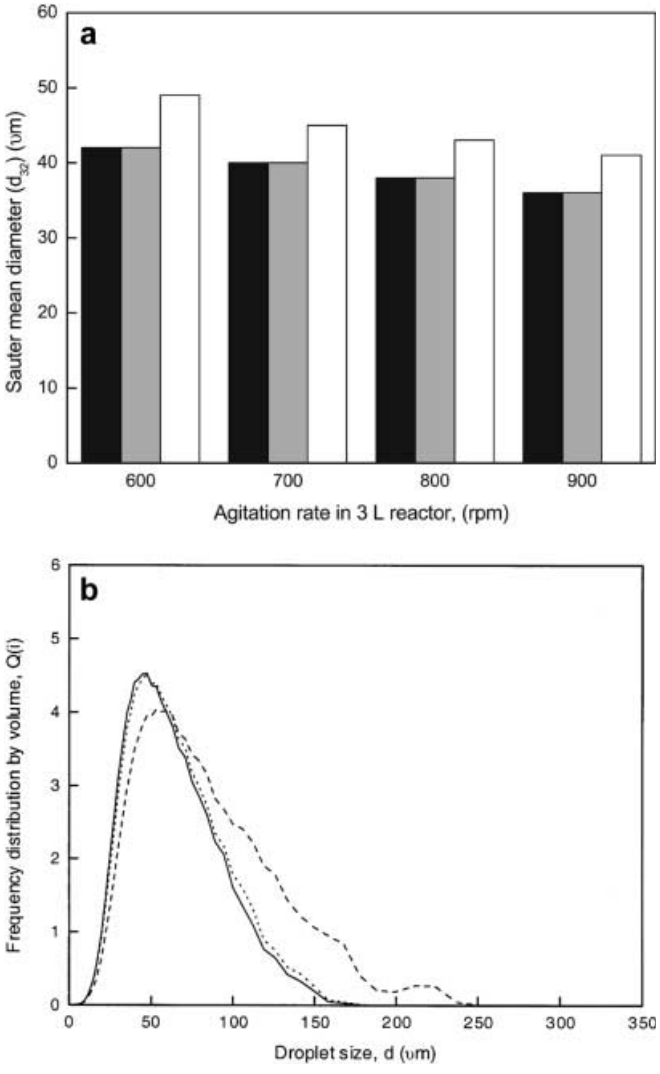

Fig. 5. **a** Sauter mean diameter (d_{32}) for a 20% v/v toluene-aqueous system in the 3-L scale-down reactor (*black bars*) and the 75-L pilot-scale reactor for scale-up under constant P/V (*grey bars*) and constant tip speed (*white bars*) criteria. **b** Droplet size frequency distribution by volume for a 20% v/v toluene-aqueous system in the absence of substrate or biomass: (__) 3-L reactor at 600 rpm; (....) 75-L reactor for scale-up using constant P/V at 305 rpm; (_ _) 75-L reactor with scale-up using constant tip speed criterion at 218 rpm

Figure 5a compares the Sauter mean drop diameters measured in the small and large reactors using both scale-up criteria with the 'clean' system. Note that on the horizontal axis the agitation rates in the 3-L reactor are shown. It is apparent that scale-up on the basis of constant power input per unit volume is the best criterion for maintenance of interfacial area at the 75-L scale when considering mean drop size. In this case, d_{32} values are found to be almost identical to those determined in the 3-L scale-down reactor for power inputs between 0.38 and 1.28 kW×m^{-3}. Scale-up on the basis of constant tip speed produced larger mean drop sizes than in the 3-L reactor in all cases (the corresponding power input values were between 0.14 and 0.45 kW×m^{-3}). This could be due to an increase in circulation time and/or the decrease in average energy dissipation rate in the larger reactor. The finding that constant power input per unit volume provides the best scale-up criterion is in agreement with the early work by van Heuven and Beek [28] and more recent work by Baldyga and co-workers [13, 27]. The latter showed that for non-coalescing systems, scale-up on the basis of constant power input per unit volume is better than constant tip speed and will result in a similar or smaller mean drop size. Other early studies, however, have suggested that constant tip speed is the most appropriate scale-up criterion [12, 29]. Clearly, more detailed studies are required, with a wider range of phase physical properties and dispersed-phase volume fractions and other factors like the average circulation time [13] may need to be included.

Figure 5b shows how the drop size distribution measured in the 3-L reactor, at an agitation rate of 600 rpm, compares to the equivalent distributions in the 75-L reactor for each of the scale-up criteria investigated. The distribution obtained in the larger reactor for scale-up on the basis of constant P/V is virtually identical to that found in the 3-L vessel. In contrast, the constant tip speed results show a distribution that is much wider and has a tail of larger drop sizes compared to that in the smaller reactor or for scale-up on the basis of constant P/V. Similar distributions were also obtained at the higher agitation rates investigated (data not shown), although the differences observed with the tip speed results were found to be less with increasing impeller speeds. When biomass was present in the system, scale-up based on constant P/V again gave average drop sizes and size distributions closer to the 3-L reactor than when constant tip speed was used. All of the drop size distributions obtained in the 75-L reactor were again adequately described by a log-normal distribution.

Finally, Fig. 6 shows the Sauter mean drop diameters determined from the drop size distribution data obtained in the 75-L reactor for both the 'clean' and biomass-containing phase systems. The trends are similar to those found at the 3-L scale (Fig. 4) with d_{32} values decreasing with increasing impeller speed and the mean drop sizes obtained in the system with 10 g_{ww}×L^{-1} of biomass present being around 25% smaller than those in the 'clean' phase system. Figure 6 also shows the predicted d_{32} values obtained using the various correlations described in Table 1 again adjusted to take account of the difference in power input as described in Sect. 3.3.1. As also found at the 3-L scale (Fig. 4), the Chen and Middleman correlation [25] was the most appropriate for the 'clean' phase system, overpredicting d_{32} values by 25–118%. The Godfrey and Grilc correlation [26] was again the most appropriate for the system with biomass present, underpredicting d_{32} values by 38–65%. Predictions from both correlations again show the closest agreement with the experimental values at the highest agitation rates used.

4 Conclusions

Maintenance of interfacial area is one of the key requirements for successful and reproducible scale-up of two-liquid phase biotransformation processes. This work demonstrates that constant power input per unit volume appears to be the best basis for predictive scale-up using both 'clean' phase systems and ones containing resting

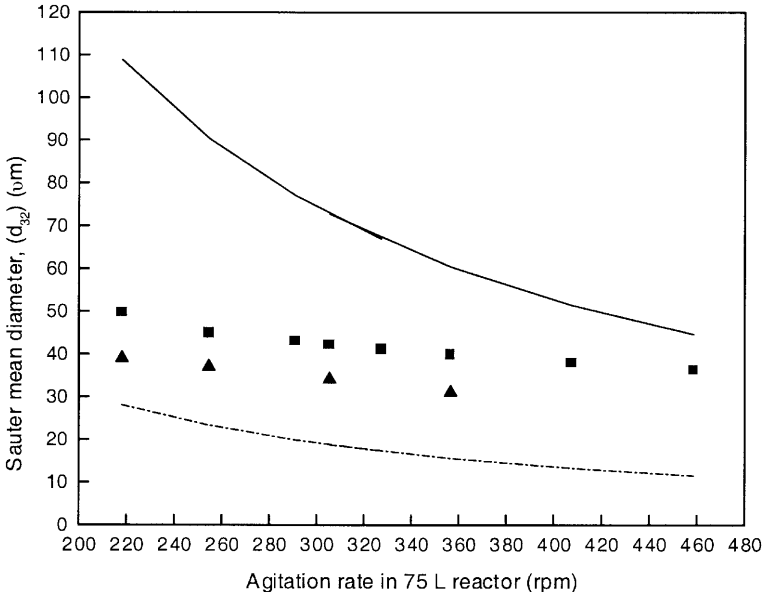

Fig. 6. Sauter mean diameter (d_{32}) against agitation rate in 20% v/v toluene-aqueous systems in the 75-L reactor (■) without biomass present and (▲) with 10 $g_{ww} \times L^{-1}$ biomass present. *Lines* show predicted d_{32} values using correlations from Table 1 corrected for increased power input: (*solid line*) Chen and Middleman [25] predictions for the biomass-free system; (*dashed line*) Godfrey and Grilc [26] predictions for the biomass-containing system

whole-cell biocatalysts. For both types of phase system, Sauter mean drop diameters and drop size distributions were very similar for scale-up on this basis from 3-L to 75-L scale in geometrically similar reactors. In all cases the drop size distributions obtained were log-normal and the Sauter mean droplet diameters could be adequately predicted by available literature correlations.

The results presented in this work were obviously obtained in a particular bioreactor geometry for a specific phase system comprising 20% v/v toluene dispersed in an aqueous buffer containing up to 10 $g_{ww} \times L^{-1}$ of a *Rhodococcus* R312 biocatalyst. While we would expect the general trends observed to apply to a range of bioconversion processes, the actual magnitude of the Sauter mean drop diameters obtained, and hence the interfacial area available for solute mass transfer, will obviously be system specific. In this respect, the scale-down methodology demonstrated here would allow the rapid experimental evaluation of specific systems using the minimum quantity of substrate and biocatalyst with a 25-fold reduction in scale. In this way, problems that might be encountered at the large scale, due to carry over of antifoam from the fermentation stage or the release of surface-active cellular components due to cell lysis, could be rapidly and efficiently identified. Our current work is examining the kinetics of this *Rhodococcus* R312 two-phase biotransformation process at the 3-L and 75-L scales.

References

1. Lilly MD, Woodley JM (1985) Biocatalytic reactions involving water-insoluble organic compounds. In: Tramper J, Plas HC Van der, Linko P (eds) Biocatalysts in Organic Syntheses. Elsevier, Amsterdam, pp 179–192
2. Lye GJ, Woodley JM (2001) Advances in the selection and design of two-liquid phase biocatalytic reactors. In: Cabral JMS, Mota M, Tramper J (eds) Multiphase Bioreactor Design. Taylor & Francis, New York, pp 115–134
3. Zhou G, Kresta SM (1998) Correlation of mean drop size and minimum drop size with the turbulence energy dissipation and the flow in an agitated tank. Chem Eng Sci 53:2063–2079
4. Schmid A, Kollmer A, Witholt B (1998) Effects of biosurfactant and emulsification on two-liquid phase *Pseudomonas oleovorans* cultures and cell-free emulsions containing n-decane. Enz Microb Technol 22:487–493
5. Kollmer A, Schmid A, Rudolf Rohr P von, Sonnleitner B (1999) On liquid-liquid mass transfer in two-liquid-phase fermentations. Bioprocess Eng 20:441–448
6. Kumar S, Ganvir V, Satyanand C, Kumar R, Gandhi KS (1998) Alternative mechanisms of drop breakup in stirred vessels. Chem Eng Sci 53:3269–3280
7. Hinze JO (1955) Fundamentals of the hydrodynamic mechanism of splitting in dispersion processes. AIChE J 1:289–295
8. Chesters AK (1991) The modelling of coalescence processes in fluid-liquid dispersions: a review of current understanding. Trans IChemE 69:259–270
9. Pacek AW, Man CC, Nienow AW (1998) On the Sauter mean diameter and size distributions in turbulent liquid/liquid dispersions in a stirred vessel. Chem Eng Sci 53:2005–2011
10. Doulah MS (1975) An effect of hold-up on drop sizes in liquid-liquid dispersions. Ind Eng Chem Fund 14:137–138
11. Boye AM, Lo M-YA, Shamlou PA (1996) The effect of two-liquid phase rheology on drop breakage in mechanically stirred vessels. Chem Eng Commun 143:149–167
12. Okufi S, Perez de Ortiz ES, Sawitowski, H (1990) Scale-up of liquid-liquid dispersions in stirred tanks. Can J Chem Eng 68:400–406
13. Podgorska W, Baldyga J (2001) Scale-up on the drop size distribution of liquid-liquid dispersions in agitated vessels. Chem Eng Sci 56:741–746
14. Woodley JM (1990) Stirred-tank power input for the scale-up of two-liquid phase biotransformations. In: Copping LG, Martin RE, Pickett JA, Bucks C, Bunch AW (eds) Opportunities in Biotransformations. Elsevier, New York, pp 63–66
15. Cull SG, Woodley JM, Lye GJ (2001) Process selection and characterisation for the biocatalytic hydration of poorly water-soluble aromatic dinitriles. Biocat Biotrans 19:131–154
16. Kerridge A (1995) The microbial biotransformation of nitrile compounds. PhD thesis. University of Exeter, UK
17. Cull S (2001) Process selection and design for the microbial biotransformation of poorly water-soluble nitrile compounds. PhD thesis. University of London, UK
18. Hobbel EF, Davies R, Rennie FW, Allen T, Butler LE, Waters ER, Smith JT, Sylvester RW (1991) Modern methods of on-line size analysis for particulate process streams. Part Part Syst Charact 8:29–34
19. El-Hamouz AM, Stewart AC (1996) On-line drop size distribution measurement of oil-water dispersion using a Par-Tec M300 laser backscatter instrument. SPE Int 36672:1–14
20. Rimpler S, Daniels R (1996) In situ particle sizing in highly concentrated oil-in-water emulsions. Pharm Technol Eur (October):72–80

21. Simmons MJH, Zaidi SH, Azzopardi BJ (2000) Comparison of laser-based drop-size measurement techniques and their application to dispersed liquid-liquid pipe flow. Opt Eng 39:505–509
22. Armenante PM, Chang GM (1998) Power consumption in agitated vessels provided with multiple-disk turbines. Ind Eng Chem Res 37:284–291
23. Guilinger TR, Grislingas AK, Erga O (1988) Phase inversion behavior of water-kerosene dispersions. Ind Eng Chem Res 27:978–982
24. Galindo E, Pacek AW, Nienow AW (2000) Study of drop and bubble sizes in a simulated mycelial fermentation broth of up to four phases. Biotech Bioeng 69:213–221
25. Chen HS, Middleman S (1967) Drop size distribution in agitated liquid-liquid systems. AIChE J 13:989–995
26. Godfrey JC, Grilc V (1977) Drop size and drop size distributions for liquid-liquid dispersions in agitated tanks of square cross section. In: Proceedings 2nd European Conference on Mixing, BHRA Fluid Engineering, vol C1. Cranfield, UK pp 1–20
27. Baldyga J, Bourne JR, Pacek AW, Amanullah A, Nienow AW (2001) Effects of agitation and scale-up on drop size in turbulent dispersions: allowance for intermittency. Chem Eng Sci 56:3377–3385
28. Heuven JW van, Beek WJ (1971) Power input, drop size and minimum stirrer speed for liquid-liquid dispersions in stirred vessels. In: Proceedings International Solvent Extraction Conference. SCI Publishing, London, pp 70–81
29. Fernandes JB, Sharma MM (1967) Effective interfacial area in agitated liquid-liquid contactors. Chem Eng Sci 22:1267–1282
30. Brown DE, Pitt K (1972) Drop size distribution of stirred non-coalescing liquid-liquid systems. Chem Eng Sci 27:577–583
31. Wang CY and Calabrese RV (1986) Drop breakup in turbulent stirred-tank contactors. Part II: relative influence of viscosity and interfacial tension. AIChE J 32: 667–676